



## Simultaneous blockade of interacting CK2 and EGFR pathways by tumor-targeting nanobioconjugates increases therapeutic efficacy against glioblastoma multiforme

Szu-Ting Chou<sup>a,1</sup>, Rameshwar Patil<sup>a,1</sup>, Anna Galstyan<sup>a,1</sup>, Pallavi R. Gangalum<sup>a</sup>, Webster K. Cavenee<sup>b</sup>, Frank B. Furnari<sup>b</sup>, Vladimir A. Ljubimov<sup>a,2</sup>, Alexandra Chesnokova<sup>a,3</sup>, Andrei A. Kramerov<sup>c</sup>, Hui Ding<sup>a</sup>, Vida Falahatian<sup>d</sup>, Leila Mashouf<sup>f</sup>, Irving Fox<sup>a</sup>, Keith L. Black<sup>a,e</sup>, Eggehard Holler<sup>a,e</sup>, Alexander V. Ljubimov<sup>c,e,1</sup>, Julia Y. Ljubimova<sup>a,e,\*,1</sup>

<sup>a</sup> Nanomedicine Research Center, Department of Neurosurgery, Cedars-Sinai Medical Center, Los Angeles, CA, USA

<sup>b</sup> Ludwig Institute for Cancer Research, University of California San Diego, La Jolla, CA, USA

<sup>c</sup> Regenerative Medicine Institute, Department of Biomedical Sciences, Cedars-Sinai Medical Center, Los Angeles, CA, USA

<sup>d</sup> Duke University School of Medicine, Department of Biostatistics and Bioinformatics, Clinical Research Training Program (CRTIP), Durham, NC, USA

<sup>e</sup> Samuel Oschin Comprehensive Cancer Center, Cedars-Sinai Medical Center, Los Angeles, CA, USA

<sup>f</sup> Johns Hopkins University, Baltimore, MD, USA

### ARTICLE INFO

#### Article history:

Received 16 August 2016

Received in revised form 12 October 2016

Accepted 2 November 2016

Available online 5 November 2016

#### Keywords:

Glioblastoma multiforme

Dual antisense oligonucleotide-dual antibody

nanobioconjugate

Blood-brain barrier delivery

Protein kinase CK2

EGFR/EGFRvIII

### ABSTRACT

Glioblastoma multiforme (GBM) remains the deadliest brain tumor in adults. GBM tumors are also notorious for drug and radiation resistance. To inhibit GBMs more effectively, polymeric acid-based blood-brain barrier crossing nanobioconjugates were synthesized that are delivered to the cytoplasm of cancer cells and specifically inhibit the master regulator serine/threonine protein kinase CK2 and the wild-type/mutated epidermal growth factor receptor (EGFR/EGFRvIII), which are overexpressed in gliomas according to The Cancer Genome Atlas (TCGA) GBM database. Two xenogeneic mouse models bearing intracranial human GBMs from cell lines LN229 and U87MG that expressed both CK2 and EGFR at different levels were used. Simultaneous knockdown of CK2 $\alpha$  and EGFR/EGFRvIII suppressed their downstream prosurvival signaling. Treatment also markedly reduced the expression of programmed death-ligand 1 (PD-L1), a negative regulator of cytotoxic lymphocytes. Downregulation of CK2 and EGFR also caused deactivation of heat shock protein 90 (Hsp90) co-chaperone Cdc37, which may suppress the activity of key cellular kinases. Inhibition of either target was associated with downregulation of the other target as well, which may underlie the increased efficacy of the dual nanobioconjugate that is directed against both CK2 and EGFR. Importantly, the single nanodrugs, and especially the dual nanodrug, markedly suppressed the expression of the cancer stem cell markers c-Myc, CD133, and nestin, which could contribute to the efficacy of the treatments. In both tumor models, the nanobioconjugates significantly increased (up to 2-fold) animal survival compared with the PBS-treated control group. The versatile nanobioconjugates developed in this study, with the abilities of anti-cancer drug delivery across biobarriers and the inhibition of key tumor regulators, offer a promising nanotherapeutic approach to treat GBMs, and to potentially prevent drug resistance and retard the recurrence of brain tumors.

© 2016 The Authors. Published by Elsevier B.V. This is an open access article under the CC BY-NC-ND license (<http://creativecommons.org/licenses/by-nc-nd/4.0/>).

### 1. Introduction

Glioblastoma multiforme (grade IV astrocytoma, GBM) accounts for >50% of malignant gliomas [1]. Despite the advances in GBM

management using surgery, radiation, and chemotherapy, recurrence of these tumors is very frequent, and GBM remains a fatal disease. The median survival time of GBM patients treated with radiation therapy and temozolomide (TMZ) is approximately 15 months, with <10% of the patients surviving for >5 years [2]. A key factor in the lack of significant improvement of therapeutic efficacy during the past decade is believed to be the molecular heterogeneity of GBMs. GBM progression has been associated with aberrant expression of vascular endothelial growth factor (VEGF), epidermal growth factor receptor (EGFR), platelet-derived growth factor receptor (PDGFR), phosphatase and tensin homolog deleted on chromosome 10 (PTEN), and other biomarkers [3].

\* Corresponding author at: Nanomedicine Research Center, Department of Neurosurgery, Cedars-Sinai Medical Center, 8700 Beverly Boulevard, AHSP-A8307, Los Angeles, CA 90048, USA.

E-mail address: [ljubimovaj@cshs.org](mailto:ljubimovaj@cshs.org) (J.Y. Ljubimova).

<sup>1</sup> These authors contributed equally to this manuscript.

<sup>2</sup> Present address: Department of Neurosurgery, University of South Florida, Tampa, FL, USA.

<sup>3</sup> Present address: School of Medicine, University of California Davis, Sacramento, CA, USA.

By GBM whole-genome sequencing, The Cancer Genome Atlas (TCGA) Research Network has reported that 57% of GBMs have EGFR alterations [4]. Moreover, TMZ-based treatment could activate EGFR and its autophosphorylated variant EGFRvIII, and result in drug resistance [5]. Downstream cascades of EGFR, including Ras-mitogen-activated protein (MAP) kinase, phosphatidylinositol 3-kinase (PI3K) and its downstream effector Akt kinase, and signal transducer and activator of transcription (STAT), play important roles in proliferation, survival, migration, and angiogenesis of tumor cells. However, monotherapy with the anti-EGFR monoclonal antibody (mAb) cetuximab or the small molecule inhibitor erlotinib has shown minimal survival benefit in clinical trials [6,7].

Protein kinase CK2 (formerly, casein kinase II) is a ubiquitous serine/threonine protein kinase that phosphorylates and interacts with >300 substrates involved in fundamental cellular functions. Studies have shown that overexpression of CK2 potentiates tumor growth through suppression of apoptosis, promotion of angiogenesis, and signaling through PI3K-Akt and Wnt [8]. EGFR and Wnt pathways cross-talk through CK2-mediated transactivation of  $\beta$ -catenin in human GBM [9]. In addition, the TCGA database has revealed that 34% of 537 analyzed GBMs have an amplified *CSNK2A1* gene that encodes the CK2 catalytic  $\alpha$  subunit (CK2 $\alpha$ ) [10].

In mouse tumor models, oral treatment with the small molecule CK2 inhibitor CX-4945 leads to downregulation of phosphorylated Akt, NF- $\kappa$ B, STAT3, and Notch-1 [10–12]. Whereas CX-4945 is currently being investigated in clinical trials ([clinicaltrials.gov](http://clinicaltrials.gov)), it is anticipated that gene therapy agents such as small interfering RNAs (siRNAs) or anti-sense oligonucleotides (AONs) can be used to target CK2 more specifically. Additionally, acquisition of tumor resistance to CX-4945 has been reported [13]. Recently, tenfibgen nanoparticles for the delivery of CK2 siRNA to head and neck cancers have been developed [14]. In a xenograft model of hypopharyngeal squamous cell carcinoma, 50% of treated mice survived for >6 months after 2 systemic administrations of the nanoparticles at a dose of 0.01 mg/kg. Although these nanoparticles are tumor-targeted, they might not readily pass through the blood brain barrier (BBB), a necessary property for reaching brain tumors.

To effectively inhibit brain tumor growth, it is important to deliver anti-cancer agents through biological barriers, including the BBB, that are largely impenetrable to therapeutic antibodies and other large molecules. To address this challenge, nanobioconjugates to inhibit intracranial GBMs in two mouse models have been created and synthesized in this study. The nanobioconjugates presented here for cancer treatment are novel nanotherapeutics in which all moieties are covalently connected to poly( $\beta$ -L-malic acid) (PMLA) and are sequentially functional in cancer cells. Our biodegradable and non-toxic nanodrugs bind to the receptors enriched on tumor vasculature and are able to cross the BBB by transcytosis. Then, they specifically bind to cancer cells and after internalization exit to the tumor cell cytoplasm from endosomes using pH-sensitive endosomal disruption unit. These structural and functional advantages make these nanobioconjugates different from classical leaky and generally untargeted drug-encapsulating nanoparticles such as liposomes or micelles [15–19].

These PMLA-based nanobioconjugates have a covalently conjugated anti-transferrin receptor (a-TfR) mAb to target tumor vasculature and allow the nanobioconjugate to be transcytosed through the BBB [17–19]. After crossing the BBB, the nanobioconjugates need to be delivered specifically to the EGFR-overexpressing GBM cells. To this end, the anti-EGFR mAb cetuximab was attached to the nanoplatfrom to facilitate the crossing through the second biobarrier, the cancer cell membrane, and deliver the inhibitors to the cytoplasm of the cancer cells. Morpholino AONs against both CK2 $\alpha$  (a catalytic subunit) and EGFR/EGFRvIII are also attached to the nanobioconjugate for specific inhibition of expression of aberrant tumor genes. This study demonstrated that tumor delivery of EGFR and CK2 $\alpha$  AONs or their co-delivery led to a significant increase of animal survival in two xenogeneic GBM mouse models, with significant reductions in several signaling proteins important for

tumor cell proliferation and invasion. Additionally, these nanodrugs were able to dramatically decrease the expression of several cancer stem cell markers. To our knowledge, these are the first nanobioconjugates that have been used to inhibit several pathways that converge on cross-regulating EGFR and CK2. The data suggest that inhibition of EGFR and/or CK2 with PMLA-based BBB-crossing nanobioconjugates is a promising therapeutic strategy for GBM.

## 2. Materials and methods

### 2.1. Cell lines and animals

Human glioblastoma cell lines LN229 and U87MG were obtained from the laboratories of W.K.C. and F.B.F. The cell lines were authenticated by the American Type Culture Collection (ATCC) on March 1, 2016 using the short tandem repeat (STR) method. LN229 cells were 100% identical to those in the ATCC database. U87MG were 93% identical, with the only difference being related to gender (female rather than male). This difference may be attributed to either the primer site mutation or uncertain gender origin acknowledged by ATCC. Cells were cultured in Dulbecco's modified Eagle medium (DMEM) containing 10% fetal bovine serum (FBS), with penicillin (100 units/mL), streptomycin (100  $\mu$ g/mL), and amphotericin B (0.25  $\mu$ g/mL), at 37 °C with 5% CO<sub>2</sub>. Female athymic NCr-nu/nu mice (6–8 weeks old) were obtained from the National Cancer Institute (NCI) at Frederick (Frederick, Maryland, USA).

### 2.2. Synthesis of PMLA nanobioconjugates

The synthesis of PMLA-based nanobioconjugates depicted schematically in Fig. 1A was performed in two major steps (Fig. 1B). In the first step, an intermediate (preconjugate) was prepared. Briefly, pendant carboxylates of PMLA were converted into an activated ester by condensing with N-hydroxysuccinimide (NHS) in the presence of dicyclohexylcarbodiimide (DCC), followed by sequential replacement of the activated ester through amide formation with mPEG5000-NH<sub>2</sub> (methoxy polyethylene glycol [mPEG], 5 Mol-% with regard to malyl units), leucine ethyl ester (LOEt, 40 Mol-% with regard to malyl units), and 2-mercaptoethylamine (2-MEA, 5 Mol-% with regard to malyl units). Mol-% of each component was calculated based on the total moles of pendant carboxylates in the PMLA, which is 100% before the attachment of any component. During the synthesis, known mole amounts of each component such as LOEt, AON, mAb, or mPEG were precisely added. Percentage (%) of the nanobioconjugate loading was calculated using the formula % = (mol component) / (mol malic acid)  $\times$  100. Each addition of a reagent was followed by the addition of an equivalent amount of triethylamine (TEA). To avoid any internal disulfide formation, 2-MEA was added together with equimolar amounts of dithiothreitol (DTT). At this stage, the preconjugate is purified and can be stored at –20 °C for several months without any loss of chemical activity.

In the second step, antibodies were attached by thioether formation after introducing PEG-maleimide (PEG-MAL) linkers by known procedures [18] followed by thiol reactive AONs to form disulfide linkages. The thiol-reactive morpholino AONs (3' amine modified) were prepared by the reaction of the amino terminus with the N-succinimidyl 3-(2-pyridyldithio) propionate (SPDP) cross-linker and purified by Sephadex LH-20 or PD-10 columns as described earlier [19]. The antibody and AON-containing nanobioconjugates were concentrated and purified over Sephadex G-75 columns.

The physicochemical characterizations of the nanobioconjugates (Supplemental Table S1) were performed by reversed phase high performance liquid chromatography (HPLC; AONs), size exclusion chromatography - HPLC (SEC-HPLC) and a Zetasizer Nano ZS90 (Malvern Instruments Ltd., Malvern, UK). All analytical methods for the nanobioconjugate characterization were used as described earlier [18].

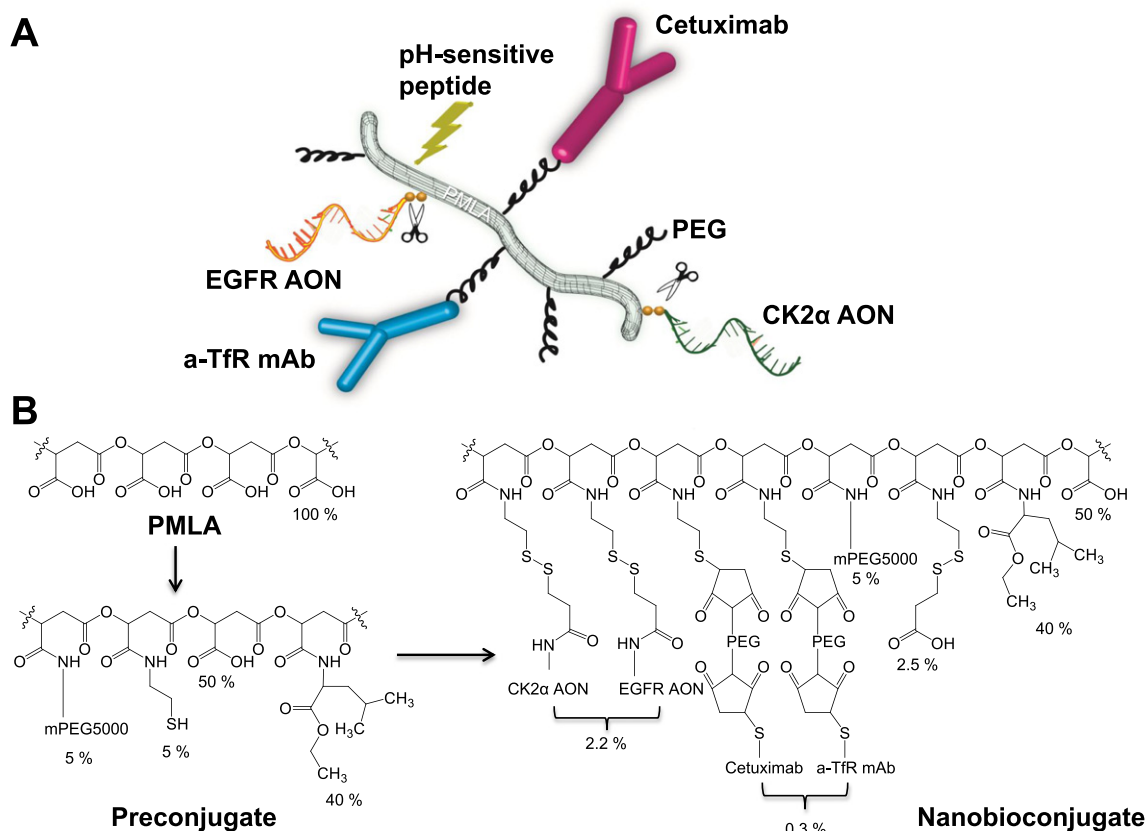


**Fig. 1.** Multifunctional nanobioconjugates used to treat glioblastoma multiforme (GBM). A) Schematic structure of the complete nanobioconjugate showing functional moieties. PMLA - poly( $\beta$ -L-malic acid), EGFR - epidermal growth factor receptor, AON - antisense oligonucleotide, PEG - polyethylene glycol, a-TfR - anti-mouse transferrin receptor to cross the BBB by transcytosis, mAb - monoclonal antibody, Cetuximab - anti-human EGFR antibody to target tumor cells, CK2 $\alpha$  - catalytic  $\alpha$  subunit of protein kinase CK2. Scissors denote AON S-S sites of cleavage from PMLA by cytoplasmic glutathione. B) Chemical synthesis of nanobioconjugate from PMLA through the preconjugate stage to the complete nanobioconjugate. Percentage contents of functional units are shown. mPEG - methoxy polyethylene glycol.

### 2.3. Reagents

PMLA was produced from the culture broth of *Physarum polycephalum* [18] and purified over Sephadex G-25. The following AONs were custom-synthesized by Gene Tools (Philomath, OR, USA): Morpholino-3'-NH<sub>2</sub> AON1 (5'-CGGACAAAGCTGGACTTGATGTTT-3') and AON2 (5'-CCTGCTTGGCACGGGTCCCGACAT-3') both targeting CK2 $\alpha$  but not a related chain CK2 $\alpha'$ , and 5'-TCGCTCCGGCTCTCCCGATCAATAC-3' targeting both the wild-type EGFR and the EGFRvIII variant [20]. Negative control AONs were as follows: standard Gene Tools AON control (5'-CCTCTTACCTCAGTTACAATTTATA-3'); unrelated AON to MMP-10 (5'-GCATCATTCTCACTGCCCTTACCTT-3'); and AON having two mismatches with CK2 $\alpha$  (5'-CAGACAAAGCTGAACTTGATGTTT-3'). Rat anti-mouse TfR/CD71 mAb (clone R17217) and anti-human EGFR chimeric (mouse/human) mAb cetuximab were purchased from BioLegend (San Diego, CA, USA) and Bristol-Myers Squibb (New York, NY, USA), respectively. Unless otherwise specified, all chemicals and solvents of highest purity were purchased from Sigma-Aldrich (St. Louis, MO, USA).

### 2.4. In vitro gene inhibition by AONs

LN229 or U87MG cells were seeded in 6-well plates at 24 h before treatment. To determine the efficacy of gene inhibition, Endo-Porter (4–6  $\mu$ M; Gene Tools) and PMLA were used to deliver CK2 $\alpha$  and EGFR AONs at doses of 5–10  $\mu$ M. The treatments with phosphate-buffered saline (PBS), Endo-Porter alone and three unrelated AONs were used as negative controls. The cells were maintained in DMEM (5% FBS)

containing Endo-Porter/AON or PMLA-AON nanobioconjugates for 66 h or 96 h, respectively. Proteins were then extracted from cell lysates using T-PER Tissue Protein Extraction Reagent (Thermo Fisher Scientific, New York, NY, USA) buffer supplemented with phosphatase and cOmplete Mini protease inhibitor cocktail (Roche, Indianapolis, IN, USA) for western blot analysis.

### 2.5. Intracranial tumor models and treatment with nanobioconjugates

All animal experiments were performed according to the guidelines of the Institutional Animal Care and Use Committee (IACUC) at Cedars-Sinai Medical Center (Los Angeles, CA, USA). LN229 cells ( $5 \times 10^5$  cells in a volume of 2  $\mu$ L) or U87MG cells ( $2.5 \times 10^4$  cells in a volume of 2  $\mu$ L) were implanted intracranially into the right basal ganglia of athymic nude mice. Three days after cell inoculation, 24 mice per cell line were randomized into 4 groups and were treated with either PBS, P/Cetu/CK2 $\alpha$  [PMLA/PEG(5%)/LOEt(40%)/a-TfR(0.15%)/Cetuximab(0.15%)/CK2 $\alpha$ -AON(2.2%)], P/Cetu/EGFR [PMLA/PEG(5%)/LOEt(40%)/a-TfR(0.15%)/Cetuximab(0.15%)/EGFR-AON(2.2%)], or P/Cetu/EGFR/CK2 $\alpha$  [PMLA/PEG(5%)/LOEt(40%)/a-TfR(0.15%)/Cetuximab(0.15%)/EGFR-AON/CK2 $\alpha$ -AON(2.2%)]. P refers to poly( $\beta$ -L-malic acid, PMLA), Cetu to anti-human EGFR mAb cetuximab to target human cancer cells, a-TfR to mouse anti-transferrin receptor mAb to cross the mouse BBB, and AON to antisense. The nanobioconjugates were injected intravenously, twice a week for 3 weeks, at a dose of 5 mg/kg of AON. When IACUC-approved endpoints were reached, anesthetized mice were euthanized by cervical dislocation followed by decapitation. Their brains

were harvested and frozen in optimal cutting temperature (OCT) compound (Sakura Finetek USA, Torrance, CA, USA).

### 2.6. Western blot analysis

Following the determination of tumor margin with hematoxylin and eosin staining, protein was extracted from OCT-embedded tissue using T-PER buffer (Thermo Fisher Scientific) supplemented with phosphatase and cOmplete Mini protease inhibitor cocktail (Roche). Protein concentration was determined by the bicinchoninic acid (BCA) method (Pierce, Rockford, IL, USA). Six micrograms of protein extract were loaded on a NuPAGE Novex 4–12% Bis-Tris gel (Thermo Fisher Scientific) and transferred to nitrocellulose membranes. The membranes were blocked in Odyssey Blocking Buffer (LI-COR Biosciences, Lincoln, NE, USA) and probed with primary and secondary antibodies. Primary antibodies against CK2 $\alpha/\alpha'$  (1:500, clone 1 AD9, Santa Cruz Biotechnology, Dallas, TX, USA), EGFR (clone D38B1), phosphorylated Akt (clone D9E), Akt (clone 40D4), c-Myc (clone D84C12), phosphorylated Cdc37 (clone D8P8F), PD-L1 (clone E1L3N), and glyceraldehyde 3-phosphate dehydrogenase (GAPDH; clone 14C10) (all at 1:1000, Cell Signaling Technology, Inc., Beverly, MA, USA) were applied overnight at 4 °C in separate reactions. The secondary antibodies used were anti-mouse IRDye 700- or anti-rabbit IRDye 800-labeled (LI-COR Biosciences). The membranes were imaged using an IR-excited fluorescence system (Odyssey CLx) and the band intensities were quantified using Image Studio 4.0 software (both from LI-COR Biosciences).

### 2.7. Immunostaining

Frozen tissue blocks were sectioned at 7–10  $\mu\text{m}$  thickness using a Leica CM3050 S cryostat (Leica Biosystems, Inc., Buffalo Grove, IL, USA). When ready for staining, tissue sections were air-dried at room temperature, fixed with ice-cold acetone for 10 min or 1% paraformaldehyde for 5 min, and then rinsed three times with PBS. Sections were incubated in a humidified chamber with blocking buffer (4% normal goat serum, 4% normal donkey serum, 1% BSA and 0.1% Triton X-100 in PBS) for 1 h at room temperature to block non-specific interactions. Non-specific binding induced by endogenous mouse immunoglobulin was blocked by Vector M.O.M. Blocking Reagent (Vector Laboratories, Burlingame, CA, USA). The blocked sections were incubated overnight at 4 °C with primary antibodies diluted in staining buffer, and later washed with PBS. Secondary antibodies for labeling were incubated for 1 h and sections mounted with ProLong Gold Antifade (Thermo Fisher Scientific) mounting medium containing 4',6-diamidino-2-phenylindole (DAPI) to counterstain cell nuclei. The samples were stained for CK2 $\alpha/\alpha'$  (clone 1 AD9, Santa Cruz Biotechnology), EGFR (clone ICR10, Abcam, Cambridge, MA, USA), EGFRvIII (clone L8A4, Absolute Antibody Ltd., Cleveland, UK), and the cancer stem cell markers: c-Myc (clone 9E10, Abcam), Nestin (clone rat-401, EMD Millipore, Temecula, CA, USA), and CD133 (clone 17A6.1, EMD Millipore). Anti-mouse IgG TRITC and anti-rat IgG FITC (both from Jackson ImmunoResearch Laboratories, Inc., West Grove, PA, USA), and anti-mouse IgG FITC (EMD Millipore) were used as secondary antibodies. Images were captured using a Leica DM6000 B microscope (Leica Microsystems, Inc., Buffalo Grove, IL, USA).

### 2.8. Statistical analysis

Statistical analyses were performed using GraphPad Prism 6 (GraphPad Software, Inc., La Jolla, CA, USA). One-way ANOVA followed by the Dunnett post hoc test was used to analyze 3 or more groups, and the Student t test was used for 2 groups, with a significance threshold of  $P < 0.05$ . Animal survival was analyzed using the Kaplan-Meier estimate (log-rank test). All data are presented as means  $\pm$  standard error of the means (SEM).

## 3. Results

### 3.1. Inhibition of tumor markers CK2 $\alpha$ and EGFR by AONs in GBM cell lines

The expression of CK2 $\alpha$  and EGFR in GBM cell lines LN229 and U87MG was determined by western blot. Both cell lines showed specific bands, but U87MG had an elevated level of EGFR compared to LN229, whereas the CK2 $\alpha$  level was much lower in U87MG than in LN229 (Fig. 2A). The efficiency of two CK2 $\alpha$ -targeting morpholino AONs was tested in LN229 cells. Both AONs downregulated CK2 $\alpha$  in a dose-dependent manner (Fig. 2B). However, because AON1 was somewhat more effective than AON2 at both concentrations (5 and 10  $\mu\text{M}$ ), only AON1 was used further for the nanobioconjugate synthesis. Three negative control AONs did not affect the expression of CK2 $\alpha$  (Supplemental Fig. S1). The efficacy of the entire nanobioconjugates bearing CK2 $\alpha$  or EGFR AONs was further tested in both cell lines for CK2 $\alpha$  inhibition (Fig. 2C). The nanobioconjugate-attached AON against CK2 $\alpha$  (P/Cetu/CK2 $\alpha$ ) was able to inhibit the expression of CK2 $\alpha$  in LN229 and U87MG cells (Fig. 2C). In agreement with previous reports that showed CK2 downstream from EGFR activation [9,11], the conjugated AON against EGFR (P/Cetu/EGFR) also resulted in a reduction of CK2 $\alpha$  protein expression, with a similar potency to the AON against CK2 $\alpha$ . Maximum inhibition with both AONs was observed at 7.5  $\mu\text{M}$ .

### 3.2. Increased tumor-bearing animal survival and downregulation of molecular targets upon treatment with nanobioconjugates

Survival rates were examined in mice with intracranial LN229 or U87MG tumor xenografts that had been treated with nanobioconjugates with covalently attached AONs to either CK2 $\alpha$  (P/Cetu/CK2 $\alpha$ ) or EGFR (P/Cetu/EGFR) individually or to both simultaneously (P/Cetu/EGFR/CK2 $\alpha$ ) (Fig. 3A). In mice with LN229 tumors, the median survival time of PBS-treated group was 37 days. Treatment with P/Cetu/CK2 $\alpha$ , P/Cetu/EGFR, or P/Cetu/EGFR/CK2 $\alpha$  significantly prolonged median survival times vs. PBS group to 70 days ( $P = 0.001$ ), 63 days ( $P = 0.015$ ), or 75 days ( $P < 0.002$ ), respectively (Fig. 3B). In mice with U87MG tumors, the PBS-treated group had a median survival time of 34 days (Fig. 3B). Treatment with P/Cetu/CK2 $\alpha$  increased the median survival time to 48 days ( $P < 0.05$ ), whereas P/Cetu/EGFR increased survival to 50 days ( $P < 0.002$ ) and P/Cetu/EGFR/CK2 $\alpha$  to 56 days ( $P < 0.002$ ) vs. PBS group (Fig. 3B). Morphological analysis of treated tumors revealed well-developed invading tumors in the PBS-treated group, whereas nanobioconjugate-treated tumors had extensive areas of tissue necrosis (Fig. 3C; LN229).

CK2 is an important protein kinase that phosphorylates many members of EGFR downstream cascades, such as the PI3K-Akt pathway or the Ras-MEK pathway. To determine the correlation between antitumor efficacy and downregulation of targets in EGFR signaling pathways, proteins were extracted from three or more tumor specimens in each treatment group and were analyzed by western blot using GAPDH as an internal control. The treatment with P/Cetu/CK2 $\alpha$  not only reduced the CK2 $\alpha$  protein level by 30%, but it also attenuated the expression of EGFR by 50% compared with the PBS control (Fig. 4A, B). P/Cetu/EGFR-treated tumors showed downregulation of EGFR protein by 90%, but also a decrease of CK2 $\alpha$  by 65%, suggesting that there is cross-talk between EGFR and CK2. Interestingly, P/Cetu/EGFR had a greater inhibitory effect on the expression of CK2 $\alpha$  than P/Cetu/CK2 $\alpha$  (65% vs. 30%, respectively). Compared to these constructs, the nanobioconjugate that combined AONs targeting both CK2 $\alpha$  and EGFR reduced the expression of CK2 $\alpha$  and EGFR by 70% and 95%, respectively.

In addition to CK2 $\alpha$  and EGFR, the activities of their downstream effectors were also investigated. The treatment with nanobioconjugates led to reduced phosphorylation of Akt and c-Myc, which are essential for tumor growth (Fig. 4A, B). The P/Cetu/CK2 $\alpha$  modestly decreased phosphorylated/activated Akt (pAkt), but P/Cetu/EGFR significantly

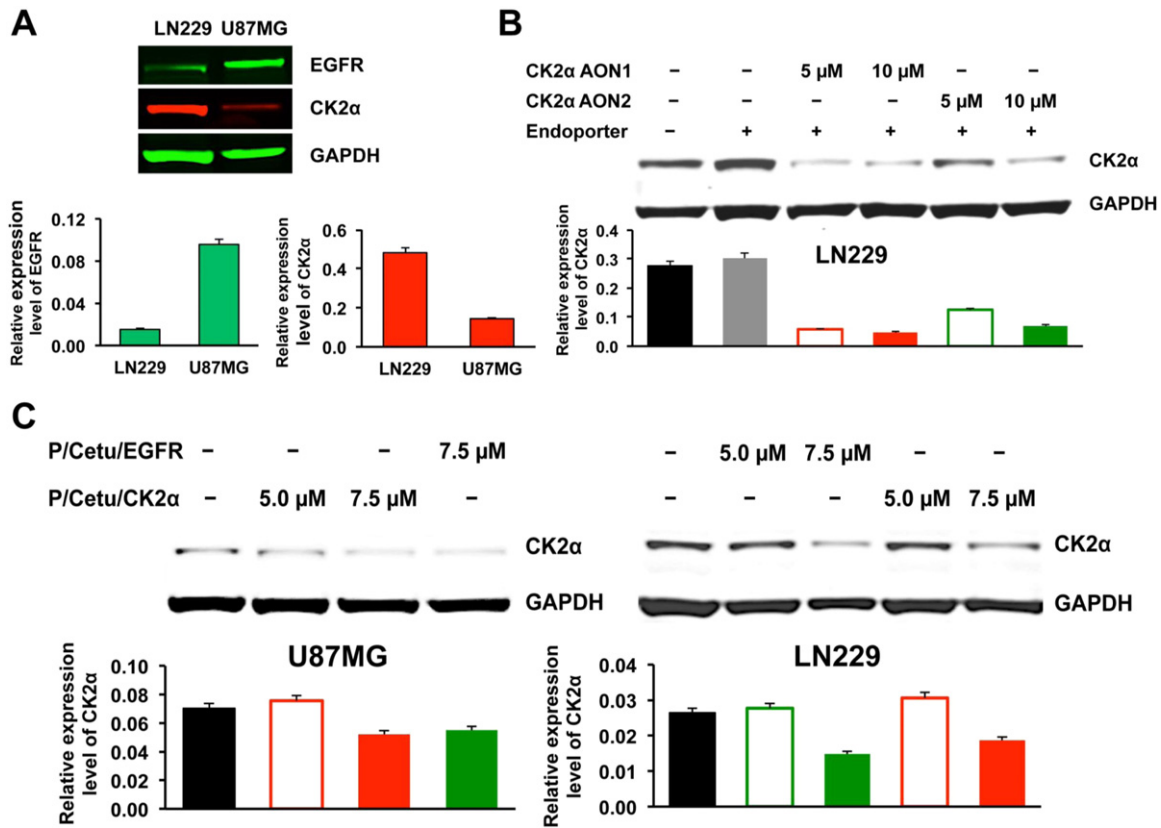


**Fig. 2.** Target protein expression and its inhibition induced by free AONs and PMLA-based nanobioconjugates. AON - antisense oligonucleotide, PMLA - poly( $\beta$ -L-malic acid). Top of each panel: western blot; bottom of each panel: quantitative evaluation. A) Expression of EGFR and CK2 $\alpha$  proteins in LN229 and U87MG cells revealed by western blot analysis with GAPDH as a housekeeping control. Note higher expression of EGFR compared to CK2 $\alpha$  in U87MG cells, with the opposite situation in LN229 cells. EGFR - epidermal growth factor receptor, CK2 $\alpha$  - catalytic  $\alpha$  subunit of protein kinase CK2, GAPDH - glyceraldehyde 3-phosphate dehydrogenase. B) Decreased expression of CK2 $\alpha$  in LN229 cells after the action of two different AONs for 4 days. CK2 $\alpha$  AON1 was significantly active at 5 and 10  $\mu$ M, whereas CK2 $\alpha$  AON2 was only active at 10  $\mu$ M. Subsequent experiments were thus conducted with only AON1. C) Efficacy of CK2 $\alpha$  inhibition in LN229 and U87MG cells was examined with nanobioconjugates containing AON1 against CK2 $\alpha$  or AON against EGFR. Both nanobioconjugates showed inhibition of CK2 $\alpha$  expression at a 7.5  $\mu$ M concentration of the conjugated AON, especially in LN229 cells. Cetu - cetuximab, P/Cetu/EGFR - nanobioconjugate with AON against EGFR, P/Cetu/CK2 $\alpha$  - nanobioconjugate with AON against CK2 $\alpha$ .

inhibited pAkt. The maximum inhibitory effect on pAkt (about 80%) was achieved with P/Cetu/EGFR/CK2 $\alpha$ . The expression of c-Myc was significantly suppressed by all three nanobioconjugates, with P/Cetu/EGFR/CK2 $\alpha$  being the most active (over 85% inhibition). Interestingly, the inhibition of heat shock protein 90 (Hsp90) co-chaperone Cdc37 observed upon all treatments positively correlated with the CK2 $\alpha$  and EGFR downregulation. This observation corroborates previous data [11,21] on the important role of Cdc37 in the regulation of CK2 and EGFR signaling. In addition, we found that programmed death-ligand 1 (PD-L1), which could suppress anti-tumor immunity, was also significantly reduced by the inhibition of EGFR and/or CK2 $\alpha$  (Fig. 4A, B).

To further validate the results of western blot, protein expression of CK2 $\alpha$  and EGFR was also examined by immunohistochemistry on mouse brain tumor cryosections (Fig. 5). Consistent with the above observations, P/Cetu/CK2 $\alpha$  and especially P/Cetu/EGFR significantly attenuated the expression of CK2 $\alpha$ , EGFR, and EGFRvIII. The combination therapy using P/Cetu/EGFR/CK2 $\alpha$  resulted in a virtually complete lack of immunostaining for these proteins (Fig. 5). Unlike the AON that was specific for only CK2 $\alpha$ , the mAb used for immunostaining also recognized the  $\alpha'$  subunit of CK2. Based on the staining patterns, it may be concluded that this subunit was also downregulated by the nanobioconjugate treatments.

### 3.3. Reduction of cancer stem cell population by nanobioconjugates

As many other tumors, gliomas comprise a cancer stem cell (CSC) population mainly responsible for tumor recurrence and poor disease prognosis [22]. These CSCs have several markers with high expression

levels correlating with decreased patient survival. Therefore, it is of major interest to monitor the tumor treatment effects on the levels of the most common CSC markers including c-Myc, CD133, and nestin [22]. Upregulated c-Myc is not only correlated with advanced malignancy and poor patient prognosis, but is also vital for the survival and self-renewal of CSCs [22]. CD133/prominin-1 is a neural progenitor marker associated with GBM invasion. Recurrent GBMs contain an increased percentage of CD133+ cells compared to the primary tumor, and many of these cells co-express nestin [22]. Nestin is a member of the intermediate filament superfamily and a stem cell marker. Its increased expression has been associated with higher-grade gliomas and lower patient survival rates [22]. For these reasons, we have used these markers to examine the effects of our treatment on CSCs.

To determine the activity of nanobioconjugates against CSCs, the pertinent markers CD133, c-Myc, and nestin were immunohistochemically detected on the tumor cryosections. As shown in Fig. 6, the inhibition of EGFR and CK2 $\alpha$ , alone or in combination, caused a dramatic reduction in immunostaining for all three markers. The combination treatment appeared to completely abolish the staining for all three markers. The data suggest that by blocking CK2 $\alpha$  and/or EGFR, CSCs can be markedly suppressed, which could translate into a lower recurrence of GBMs.

## 4. Discussion

In recent years, the concept of targeted cancer therapy has significantly changed. Common small molecule treatments target a specific tumor molecular marker to modulate its expression in a desired way but have no tissue specificity, often resulting in serious side effects

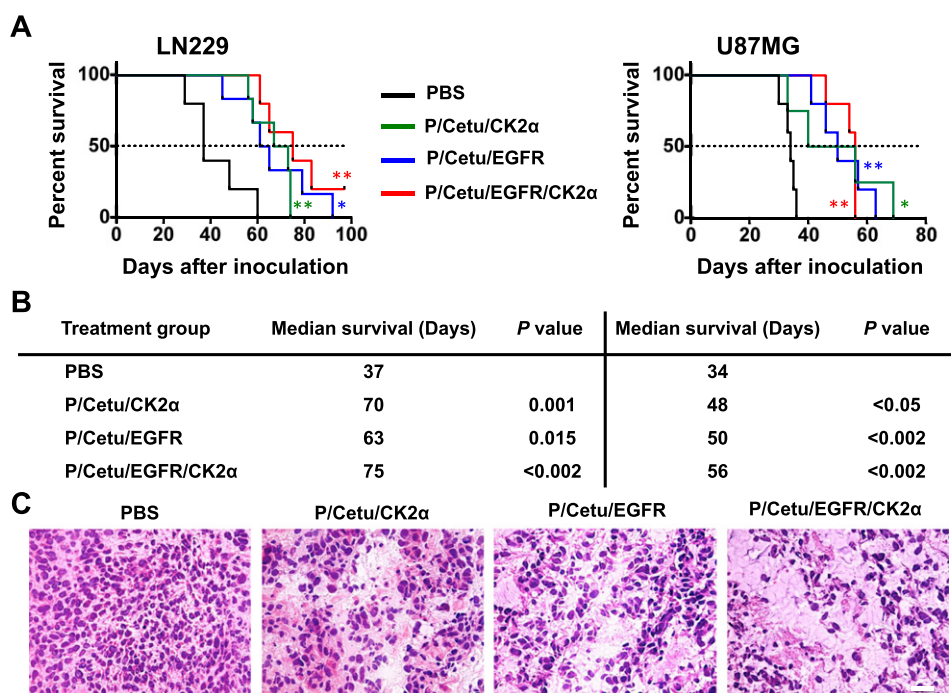


**Fig. 3.** Nanobioconjugate treatment of mice bearing intracranial LN229 and U87MG human GBM tumors. A) Kaplan-Meier survival curves (log-rank test) show significantly prolonged survival of LN229 and U87MG tumor-bearing mice upon treatment with AONs targeting CK2 $\alpha$ , EGFR, or EGFR + CK2 $\alpha$  combined on a single nanobioconjugate. The results represent means  $\pm$  SEM vs. PBS treatment. \*,  $P < 0.05$ ; \*\*,  $P < 0.01$ . AON - antisense oligonucleotide, CK2 $\alpha$  - catalytic  $\alpha$  subunit of protein kinase CK2, EGFR - epidermal growth factor receptor, PBS - phosphate-buffered saline, Cetu - cetuximab, P/Cetu/CK2 $\alpha$  - nanobioconjugate with AON against CK2 $\alpha$ , P/Cetu/EGFR - nanobioconjugate with AON against EGFR, P/Cetu/EGFR/CK2 $\alpha$  - nanobioconjugate with AONs against both EGFR and CK2 $\alpha$ . B) Median survival times (days) of the different groups of mice showed significant effects of all nanobioconjugates in both LN229 and U87MG GBMs compared with PBS-treated mice, according to the log-rank test. C) Hematoxylin and eosin staining of LN229 tumor sections after treatment. Compared with the PBS control, treatment with all nanobioconjugates resulted in the appearance of necrotic areas within the tumor and reduced the GBM cellularity. The nanobioconjugate with the combination of AONs against CK2 $\alpha$  and EGFR produced a stronger effect than single nanobioconjugates.

because they also act on normal tissues. In contrast, nanomedicine offers targeting possibility not only in terms of a specific gene/protein affected, but also in terms of acting on a specific tissue or a specific tumor, which would result in fewer side effects. Nanodrugs often enter the target cells by bypassing membrane pumps or using different mechanisms of delivery across cell membranes, thereby significantly lowering the probability of drug resistance development [23]. Additionally, next-generation nanomedicines can pass through biological barriers and offer combined drug treatment using a single delivery vehicle, enhancing the tumoricidal effect [17]. In this report, we engineered nanobioconjugate drugs that were able to pass through the BBB and deliver to intracranial tumors antisense inhibitors of key GBM markers identified from the TCGA GBM database, i.e. EGFR (both wild type and the mutated EGFRvIII) and the master regulator protein kinase CK2 [4,10]. These new nanodrugs were tested in two xenogeneic models of orthotopic intracranial human GBMs with high- and low-level expression of CK2 and EGFR.

All used nanodrugs (against either CK2 $\alpha$  or EGFR or both) were able to significantly prolong the survival of tumor-bearing animals in both GBM models, with similar results (Fig. 3). The dual nanobioconjugate (P/Cetu/EGFR/CK2 $\alpha$ ) showed a tendency for a stronger inhibiting effect towards the downstream signaling intermediates of CK2 and EGFR pathways including pAkt, pCdc37, and c-Myc, as well as PD-L1 (Fig. 4).

The LN229 glioma cell line expressed a high level of CK2 $\alpha$  and a low level of EGFR, whereas the U87MG glioma cell line had a low level of CK2 $\alpha$  and high level of EGFR in vitro (Fig. 2A). The in vivo treatment results (Fig. 3) are in line with these levels, with the anti-CK2 $\alpha$  nanodrug being more effective in LN229, whereas the anti-EGFR nanodrug was somewhat more effective in U87MG. The dual nanobioconjugate was similar to single nanodrugs in promoting animal survival for both gliomas. This may be partially explained by cross-talk between CK2 and EGFR downstream signaling [11]. It should also be noted, that the dual

nanodrug had only half of the concentration of each AON to either CK2 $\alpha$  or EGFR compared to single nanodrugs. Therefore, it allowed to substantially lowering the dose of each AON with the same anti-tumor effect. This is one of the main advantages of nanotherapy aimed at reducing drug toxicity and side effects for non-targeted tissues generally seen at higher drug doses. This nanodrug design and development could be also important for glioma treatment in the clinic when patients have a heterogeneous tumor genotype.

Noteworthy, the anti-CK2 $\alpha$  nanodrug reduced CK2 $\alpha$  protein expression by 30%, but the anti-EGFR treatment resulted in a greater inhibition (65%). Likewise, CK2 $\alpha$  inhibition also resulted in significant EGFR downregulation. This phenomenon was previously described in tumor cell cultures [11,24] and was observed here for the first time in nanodrug-treated brain tumors. There may be several mechanisms underlying this cross-inhibition. In the case of the anti-CK2 $\alpha$  nanodrug, the tumor cell-targeting anti-EGFR mAb cetuximab could contribute to partial downregulation of EGFR. A more general mechanism may involve cross-talk and convergence of downstream pathways of these two powerful signaling mediators [11]. Additionally, there is a subset of microRNAs that inhibit both CK2 $\alpha$  and EGFR (e.g., miR-211, miR-571, and miR-7110), and these are all decreased in more aggressive GBMs and lung cancers [25–27]. These findings may suggest that nanodrug inhibition of one target allows the remaining miRNA to more efficiently inhibit the other target, thereby potentiating the effect.

Treatment with P/Cetu/CK2 $\alpha$  modestly downregulated the phosphorylation of prosurvival Akt at Ser473, in agreement with earlier data using a small molecule CK2 inhibitor [28,29]. However, phosphorylation at other sites in Akt is also important for its activation by CK2 [28]. As direct EGFR targeting decreases Akt phosphorylation at Thr308 and Ser483, the dual nanobioconjugate P/Cetu/EGFR/CK2 $\alpha$  could mediate synergistic abrogation of Akt phosphorylation (Fig. 4A) at all three key residues, enhancing the anti-tumor effect. Moreover,

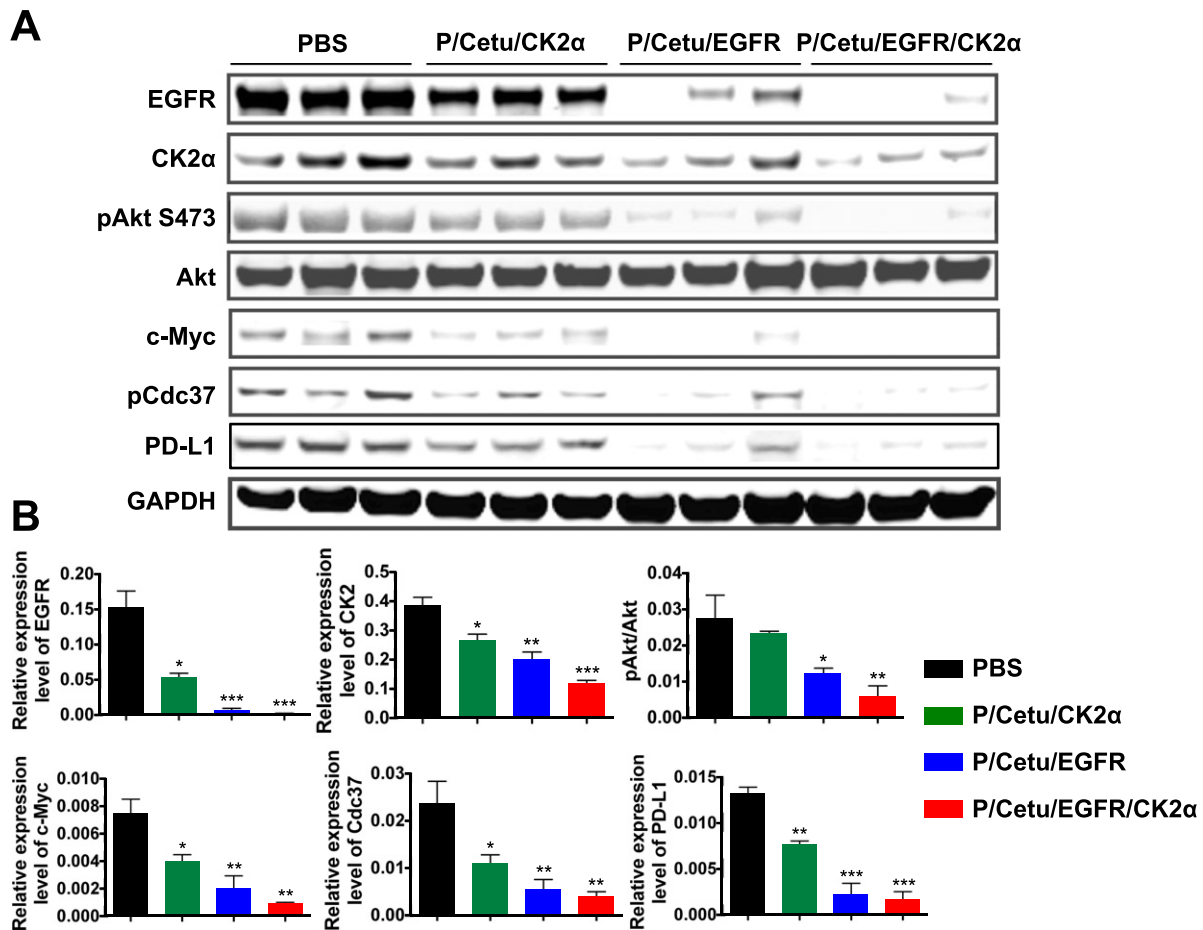


**Fig. 4.** Expression of molecular targets in xenogeneic LN229 brain tumors revealed by western blot. A) Protein expression of EGFR, CK2 $\alpha$ , phosphorylated Akt [Ser473] (pAkt S473), total Akt, c-Myc, phosphorylated Cdc37 (pCdc37), and programmed death-ligand 1 (PD-L1). Treatment with all nanobioconjugates resulted in significantly lower expression of the analyzed proteins. Three independent tumor specimens per each treatment group were analyzed. AON - antisense oligonucleotide, PBS - phosphate-buffered saline, Cetu - cetuximab, CK2 $\alpha$  - catalytic  $\alpha$  subunit of protein kinase CK2, EGFR - epidermal growth factor receptor, P/Cetu/CK2 $\alpha$  - nanobioconjugate with AON against CK2 $\alpha$ , P/Cetu/EGFR - nanobioconjugate with AON against EGFR, P/Cetu/EGFR/CK2 $\alpha$  - nanobioconjugate with AONs against both EGFR and CK2 $\alpha$ , GAPDH - glyceraldehyde 3-phosphate dehydrogenase. B) Band intensities of tumor samples were quantified by Image Studio software and normalized against GAPDH or Akt (for pAkt) as a control. All proteins showed statistically significant decreases following the treatments. Note significantly reduced expression of EGFR upon anti-CK2 $\alpha$  treatment and vice versa. The results represent means  $\pm$  SEMs vs. PBS treatment. \*,  $P < 0.05$ ; \*\*,  $P < 0.01$ ; \*\*\*,  $P < 0.001$ .

the activity and stability of Akt rely on a complex composed of Cdc37 and Hsp90 [30]. CK2 also plays a crucial role in the activation of the Hsp90/Cdc37 complex forming a positive feedback loop with Akt and other kinases. In addition to Akt, CK2-dependent phosphorylation of Cdc37 facilitates the activation of other EGFR downstream effectors including Raf and Src [31]. Blocking CK2 could thus indirectly affect EGFR signaling through downregulation of Cdc37 observed after nanobioconjugate treatment (Fig. 4A), and also through inhibition of other pathways including the PTEN-dependent pathway [32,33]. This cross-talk could also be the basis of angiogenic signaling through CK2 and EGFR [34,35].

Importantly, we have observed significant downregulation of the immune response modulator PD-L1 in treated GBMs. The PD-1/PD-L1 signaling that leads to an immunosuppressive tumor microenvironment and progressive tumor proliferation has been extensively studied [36]. The mAb nivolumab that neutralizes PD-1 is currently under investigation in clinical trials to treat multiple cancers. The expression of PD-L1/B7-H1 by glioma cells reduces the number of tumor infiltrating lymphocytes and is correlated with advanced glioma grade [37,38]. In our experiments, an 80% inhibition of PD-L1 that was observed while simultaneously targeting CK2 $\alpha$  and EGFR might be attributed to the inactivation of Akt [39]. The ability to downregulate PD-L1 makes the used nanobioconjugates appealing therapeutic agents to restore impaired anti-tumor T cell function.

An important finding in this study was a pronounced suppression of several CSC markers in GBMs upon treatment with nanobioconjugates (Figs. 4A, 6). Cancer stem cells may be mainly responsible for the GBM recurrence as they are more resistant to conventional tumor therapies [22,40,41]. CK2 is not only linked to sustained growth of GBMs, but is also involved in the maintenance of cancer stem cells through activation of Notch, Wnt/ $\beta$ -catenin, or Hedgehog/Gli1 signaling [42–45]. For instance, siRNA-mediated inhibition of CK2 is associated with decreased transcriptional activities of Gli1 and the Notch receptor intracellular domain in lung cancers [12,45]. The reduction of nestin observed upon nanobioconjugate treatment (Fig. 6) suggests that Notch signaling may be inhibited by the AON against CK2 $\alpha$  [46]. At the same time the EGFR family members and Notch signaling are deregulated in many human cancers [47].  $\beta$ -catenin that can be regulated by CK2 plays a central role in Wnt signaling. Stabilized  $\beta$ -catenin translocates to the nucleus, forming a complex with DNA-bound T cell factor/lymphoid enhancing factor to activate Wnt signaling [48]. Several groups have found that  $\beta$ -catenin is prevented from degradation by CK2-mediated phosphorylation at Thr393 [49,50]. Moreover, the interaction of CK2 $\alpha$  and ERK2 facilitates the phosphorylation of  $\alpha$ -catenin at S641, which promotes the transcriptional activity of  $\beta$ -catenin [9]. Furthermore, reduced CK2 activity leads to the inhibition of two  $\beta$ -catenin-regulated stem cell genes, *OCT4* and *NANOG*, resulting in decreased tumorigenesis and expression of the CSC marker CD133 as an indicator of GBM cell

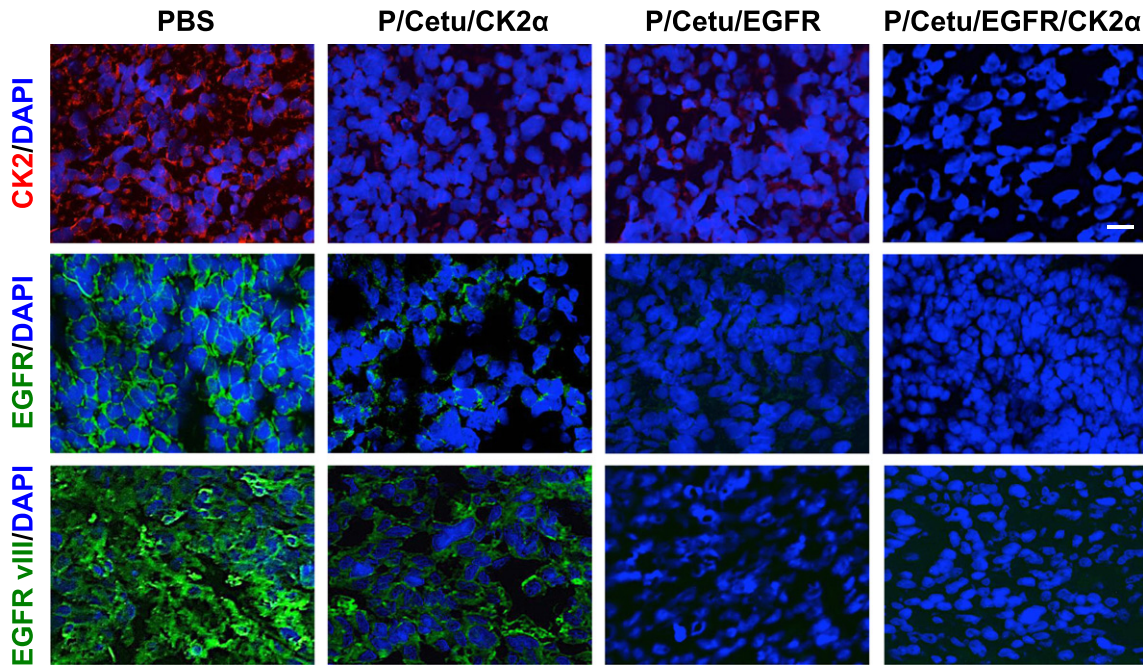


**Fig. 5.** Expression of CK2 $\alpha/\alpha'$ , EGFR, and EGFRvIII in frozen sections of LN229 tumors revealed by immunohistochemistry. Nuclei were counterstained with DAPI. The nanobioconjugates caused marked inhibition of the expression of all targets. The P/Cetu/CK2 $\alpha$  nanobioconjugate strongly inhibited the expression of CK2 and moderately inhibited the expression of EGFR and EGFRvIII. In accordance with the western blot data, the other nanobioconjugates were more effective, especially the dually targeted nanobioconjugate (P/Cetu/EGFR/CK2 $\alpha$ ). Representative pictures are shown. Scale bar = 10  $\mu$ m. AON - antisense oligonucleotide, PBS - phosphate-buffered saline, Cetu - cetuximab, CK2 $\alpha$  - catalytic  $\alpha$  subunit of protein kinase CK2, EGFR - epidermal growth factor receptor, EGFRvIII - mutated EGFR, P/Cetu/CK2 $\alpha$  - nanobioconjugate with AON against CK2 $\alpha$ , P/Cetu/EGFR - nanobioconjugate with AON against EGFR, P/Cetu/EGFR/CK2 $\alpha$  - nanobioconjugate with AONs against both EGFR and CK2 $\alpha$ .

proliferation [51]. In addition to CK2, EGFR is also involved in survival and self-renewal of GBM cancer stem cells. It was reported that EGFR or EGFRvIII activation of Akt results in phosphorylation of Smad5 and overexpression of inducer of differentiation 3 (ID3), which promotes

the emergence of glioma stem-like cells in primary astrocytes [52]. Additionally, EGFR cross-communicates with  $\beta$ -catenin through intermediates including STAT3 and Akt [53]. Interestingly, inhibition of STAT3 causes downregulation of nestin in GBMs, suggesting dependence on

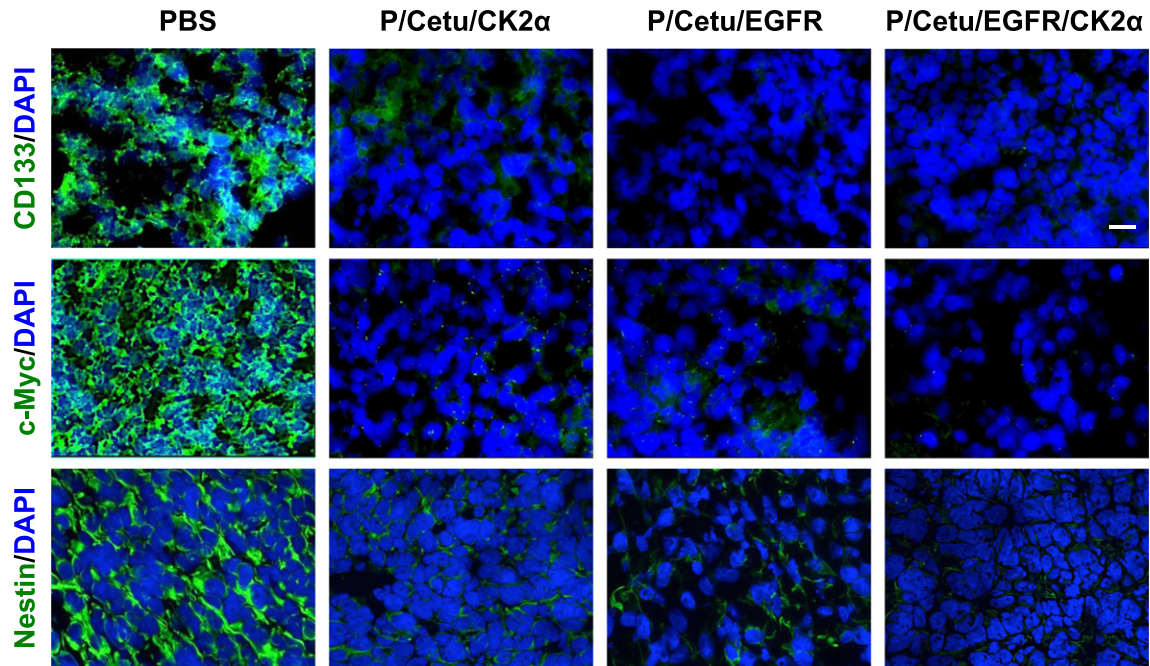


**Fig. 6.** Expression of cancer stem cell markers CD133, c-Myc, and nestin in frozen sections of LN229 tumors revealed by immunohistochemistry. Nuclei were counterstained with DAPI. All nanobioconjugates caused marked inhibition of the expression of all targets, especially the dually targeted nanobioconjugate (P/Cetu/EGFR/CK2 $\alpha$ ). Representative pictures are shown. Scale bar = 10  $\mu$ m. AON - antisense oligonucleotide, PBS - phosphate-buffered saline, Cetu - cetuximab, CK2 $\alpha$  - catalytic  $\alpha$  subunit of protein kinase CK2, EGFR - epidermal growth factor receptor, P/Cetu/CK2 $\alpha$  - nanobioconjugate with AON against CK2 $\alpha$ , P/Cetu/EGFR - nanobioconjugate with AON against EGFR, P/Cetu/EGFR/CK2 $\alpha$  - nanobioconjugate with AONs against both EGFR and CK2 $\alpha$ .



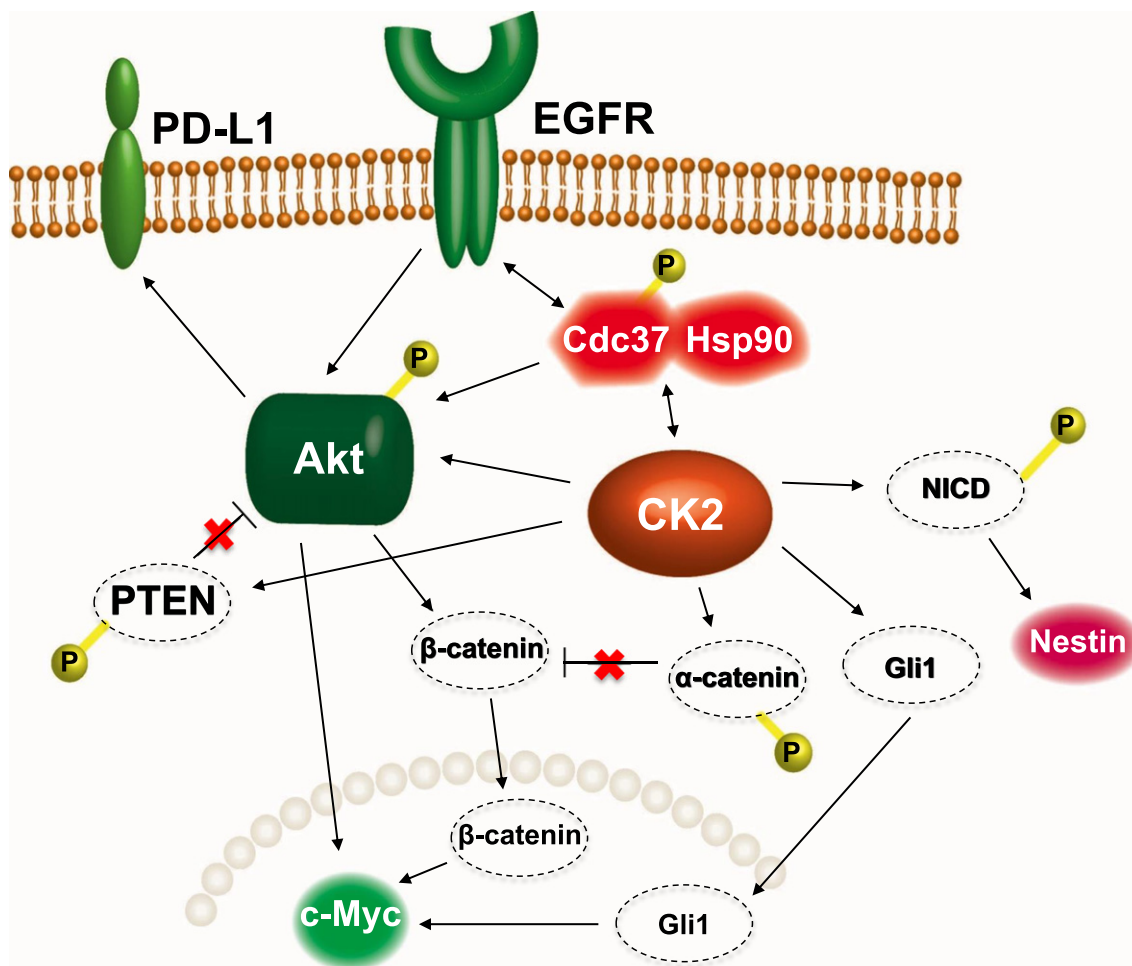


**Fig. 7.** A schematic diagram illustrating the possible interplay between the EGFR and CK2 signaling pathways that regulate GBM cell proliferation. An attached “P” indicates phosphorylation. PD-L1 - programmed death-ligand 1, EGFR - epidermal growth factor receptor, Hsp90 - heat shock protein 90, Cdc37 - co-chaperone of Hsp90, Akt - a serine/threonine protein kinase, CK2 - protein kinase CK2, NICD - intracellular domain of the Notch receptor, PTEN - tensin homolog deleted on chromosome 10, Gli1 - glioma-associated oncogene homolog 1 (zinc finger protein). Nestin and c-Myc are cancer stem cell markers important for glioma invasion. Catenins are cell-cell adhesion proteins;  $\beta$ -catenin also regulates transcription and is part of the Wnt signaling pathway that regulates cell proliferation and migration.

EGFR activation [54]. Downregulation of CSC markers in GBMs upon treatment with our nanobioconjugates may thus result from inhibition of these multiple pathways.

In summary, using two mouse models of intracranial glioma, we demonstrated significantly increased survival of tumor-bearing animals upon systemic treatment with tumor-targeted nanobioconjugates that inhibited CK2 $\alpha$  and/or EGFR. The molecular mechanisms underlying this effect (Fig. 7) may be related to the profound inhibition of several converging prosurvival signaling pathways and inhibition of the expression of several cancer stem cell markers in treated gliomas (Fig. 6). The nanobioconjugate that provided simultaneous inhibition of CK2 $\alpha$  and EGFR showed the strongest inhibition of its intended targets and downstream signaling pathways and may be further considered for translational applications, along with other new developments including immunotherapy [47].

#### Conflict of interest statement

K.L. Black, E. Holler, A.V. Ljubimov, and J.Y. Ljubimova are stockholders of Arrogene, Inc., a startup biotechnology company. K.L. Black, A.V. Ljubimov, and J.Y. Ljubimova are co-founders and E. Holler is director of chemical synthesis of Arrogene, Inc. The company did not finance any of the studies described herein. K.L. Black, E. Holler, and J.Y.

Ljubimova are listed as inventors on U.S. patent no. 8562964 concerning the design of nanobioconjugate drug delivery system with an attached antisense oligonucleotide to protein kinase CK2.

#### Acknowledgements

##### Authors' contributions

Conception and design of the study: E. Holler, A.V. Ljubimov, and J.Y. Ljubimova. Development of the methodology: S.-T. Chou, P.R. Gangalum, R. Patil, A. Galstyan, E. Holler, and J.Y. Ljubimova. Acquisition of data (including providing animals and facilities): S.-T. Chou, R. Patil, P.R. Gangalum, A. Chesnokova, A. Galstyan, V.A. Ljubimov, L. Mashouf, and I. Fox. Writing, review, and/or revision of the manuscript: S.-T. Chou, P.R. Gangalum, R. Patil, V.A. Ljubimov, V. Falahatian, E. Holler, A.V. Ljubimov, and J.Y. Ljubimova. Administrative, technical, or material support (i.e., reporting or organizing data, constructing databases, providing cell lines): W.K. Cavenee, F.B. Furnari, H. Ding, V. Falahatian, and K.L. Black. Study supervision: E. Holler, A.V. Ljubimov, and J.Y. Ljubimova.

##### Funding

This study was supported by grants from the National Institutes of Health (U01 CA151815, R01 CA136841, R01 CA188743, R01 CA209921, and R01 EY013431).

## Appendix A. Supplementary data

Supplementary data to this article can be found online at <http://dx.doi.org/10.1016/j.jconrel.2016.11.001>.

## References

- [1] J.A. Schwartzbaum, J.L. Fisher, K.D. Aldape, M. Wrensch, Epidemiology and molecular pathology of glioma, *Nat. Clin. Pract. Neurol.* 2 (2006) 494–503.
- [2] R. Stupp, W.P. Mason, M.J. van den Bent, M. Weller, B. Fisher, M.J. Taphoorn, et al., Radiotherapy plus concomitant and adjuvant temozolomide for glioblastoma, *N. Engl. J. Med.* 352 (2005) 987–996.
- [3] P.Y. Wen, S. Kesari, Malignant gliomas in adults, *N. Engl. J. Med.* 359 (2008) 492–507.
- [4] C.W. Brennan, R.G. Verhaak, A. McKenna, B. Campos, H. Nounshmehr, S.R. Salama, et al., The somatic genomic landscape of glioblastoma, *Cell* 155 (2013) 462–477.
- [5] J.L. Munoz, V. Rodriguez-Cruz, S.J. Greco, V. Nagula, K.W. Scotto, P. Rameshwar, Temozolomide induces the production of epidermal growth factor to regulate MDR1 expression in glioblastoma cells, *Mol. Cancer Ther.* 13 (2014) 2399–2411.
- [6] B. Neyns, J. Sadones, E. Joossens, F. Bouttens, L. Verbeke, J.F. Baurain, et al., Stratified phase II trial of cetuximab in patients with recurrent high-grade glioma, *Ann. Oncol.* 20 (2009) 1596–1603.
- [7] M.J. van den Bent, A.A. Brandes, R. Rampling, M.C. Kouwenhoven, J.M. Kros, A.F. Carpentier, et al., Randomized phase II trial of erlotinib versus temozolomide or carmustine in recurrent glioblastoma: EORTC brain tumor group study 26034, *J. Clin. Oncol.* 27 (2009) 1268–1274.
- [8] K. Ahmed, O.G. Issinger, R. Szyszka (Eds.), Protein kinase CK2 cellular function in normal and disease states, *Advances in Biochemistry in Health and Disease*, vol. 12, Springer International Publishers, Switzerland, 2015 (378 pp.).
- [9] H. Ji, J. Wang, H. Nika, D. Hawke, S. Keezer, Q. Ge, et al., EGF-induced ERK activation promotes CK2-mediated disassociation of  $\alpha$ -catenin from  $\beta$ -catenin and transactivation of  $\beta$ -catenin, *Mol. Cell* 36 (2009) 547–559.
- [10] Y. Zheng, B.C. McFarland, D. Drygin, H. Yu, S.L. Bellis, H. Kim, et al., Targeting protein kinase CK2 suppresses prosurvival signaling pathways and growth of glioblastoma, *Clin. Cancer Res.* 19 (2013) 6484–6494.
- [11] J. Bliesath, N. Huser, M. Omori, D. Bunag, C. Proffitt, N. Streiner, et al., Combined inhibition of EGFR and CK2 augments the attenuation of PI3K-Akt-mTOR signaling and the killing of cancer cells, *Cancer Lett.* 322 (2012) 113–118.
- [12] S. Zhang, H. Long, Y.L. Yang, Y. Wang, D. Hsieh, W. Li, et al., Inhibition of CK2 $\alpha$  down-regulates Notch1 signalling in lung cancer cells, *J. Cell. Mol. Med.* 17 (2013) 854–862.
- [13] Y. Bian, J. Han, V. Kannabiran, S. Mohan, H. Cheng, J. Friedman, et al., MEK inhibitor PD-0325901 overcomes resistance to CK2 inhibitor CX-4945 and exhibits anti-tumor activity in head and neck cancer, *Int. J. Biol. Sci.* 11 (2015) 411–422.
- [14] G.M. Unger, B.T. Kren, V.L. Korman, T.G. Kimbrough, R.I. Vogel, F.G. Ondrey, et al., Mechanism and efficacy of sub-50-nm tenfibgen nanocapsules for cancer cell-directed delivery of anti-CK2 RNAi to primary and metastatic squamous cell carcinoma, *Mol. Cancer Ther.* 13 (2014) 2018–2029.
- [15] T.M. Allen, L.G. Cleland, Serum-induced leakage of liposome contents, *Biochim. Biophys. Acta* 597 (1980) 418–426.
- [16] R. Savič, T. Azzam, A. Eisenberg, D. Maysinger, Assessment of the integrity of poly(caprolactone)-*b*-poly(ethylene oxide) micelles under biological conditions: a fluorogenic-based approach, *Langmuir* 22 (2006) 3570–3578.
- [17] H. Ding, S. Inoue, A.V. Ljubimov, R. Patil, J. Portilla-Arias, J. Hu, et al., Inhibition of brain tumor growth by intravenous poly( $\beta$ -L-malic acid) nanobiocjugate with pH-dependent drug release, *Proc. Natl. Acad. Sci. U. S. A.* 107 (2010) 18143–18148.
- [18] J.Y. Ljubimova, H. Ding, J. Portilla-Arias, R. Patil, P.R. Gangalum, A. Chesnokova, et al., Polymalic acid-based nano biopolymers for targeting of multiple tumor markers: an opportunity for personalized medicine? *J. Vis. Exp.* 88 (2014) e50668.
- [19] R. Patil, A.V. Ljubimov, P.R. Gangalum, H. Ding, J. Portilla-Arias, S. Wagner, et al., MRI virtual biopsy and treatment of brain metastatic tumors with targeted nanobiocjugates: nanoclinic in the brain, *ACS Nano* 9 (2015) 5594–5608.
- [20] S. Inoue, R. Patil, J. Portilla-Arias, H. Ding, B. Konda, A. Espinoza, et al., Nanobiopolymer for direct targeting and inhibition of EGFR expression in triple negative breast cancer, *PLoS One* 7 (2012) e31070.
- [21] Y. Miyata, Protein kinase CK2 in health and disease: CK2: the kinase controlling the Hsp90 chaperone machinery, *Cell. Mol. Life Sci.* 66 (2009) 1840–1849.
- [22] A. Bradshaw, A. Wickremsekera, S.T. Tan, L. Peng, P.F. Davis, T. Itinteang, Cancer stem cell hierarchy in glioblastoma multiforme, *Front. Surg.* 3 (2016) 21.
- [23] J.L. Markman, A. Rekechenetskiy, E. Holler, J.Y. Ljubimova, Nanomedicine therapeutic approaches to overcome cancer drug resistance, *Adv. Drug Deliv. Rev.* 65 (2013) 1866–1879.
- [24] B. Guerra, M. Fischer, S. Schaefer, O.G. Issinger, The kinase inhibitor D11 induces caspase-mediated cell death in cancer cells resistant to chemotherapeutic treatment, *J. Exp. Clin. Cancer Res.* 34 (2015) 125.
- [25] S. Asuthkar, K.K. Velpula, C. Chetty, B. Gorantla, J.S. Rao, Epigenetic regulation of miRNA-211 by MMP-9 governs glioma cell apoptosis, chemosensitivity and radiosensitivity, *Oncotarget* 3 (2012) 1439–1454.
- [26] E.C. Park, G. Kim, J. Jung, K. Wang, S. Lee, S.S. Jeon, et al., Differential expression of MicroRNAs in patients with glioblastoma after concomitant chemoradiotherapy, *OMICS* 17 (2013) 259–268.
- [27] Q.Y. Chen, D.M. Jiao, Y. Zhu, H. Hu, J. Wang, X. Tang, et al., Identification of carcinogenic potential-associated molecular mechanisms in CD133<sup>+</sup> A549 cells based on microRNA profiles, *Tumour Biol.* 37 (2016) 521–530.
- [28] G. Di Maira, M. Salvi, G. Arrighoni, O. Marin, S. Sarno, F. Brustolon, et al., Protein kinase CK2 phosphorylates and upregulates Akt/PKB, *Cell Death Differ.* 12 (2005) 668–677.
- [29] F. Pierre, P.C. Chua, S.E. O'Brien, A. Siddiqui-Jain, P. Bourbon, M. Haddach, et al., Pre-clinical characterization of CX-4945, a potent and selective small molecule inhibitor of CK2 for the treatment of cancer, *Mol. Cell. Biochem.* 356 (2011) 37–43.
- [30] A.D. Basso, D.B. Solit, G. Chiosis, B. Giri, P. Tschlis, N. Rosen, Akt forms an intracellular complex with heat shock protein 90 (Hsp90) and Cdc37 and is destabilized by inhibitors of Hsp90 function, *J. Biol. Chem.* 277 (2002) 39858–39866.
- [31] Y. Miyata, E. Nishida, CK2 controls multiple protein kinases by phosphorylating a kinase-targeting molecular chaperone, Cdc37, *Mol. Cell. Biol.* 24 (2004) 4065–4074.
- [32] A.M. Al-Khouri, Y. Ma, S.H. Togo, S. Williams, T. Mustelin, Cooperative phosphorylation of the tumor suppressor phosphatase and tensin homologue (PTEN) by casein kinases and glycogen synthase kinase 3 $\beta$ , *J. Biol. Chem.* 280 (2005) 35195–35202.
- [33] S.J. Miller, D.Y. Lou, D.C. Seldin, W.S. Lane, B.G. Neel, Direct identification of PTEN phosphorylation sites, *FEBS Lett.* 528 (2002) 145–153.
- [34] A.A. Kramerov, M. Saghizadeh, S. Caballero, L.C. Shaw, S. Li Calzi, M. Bretner, et al., Inhibition of protein kinase CK2 suppresses angiogenesis and hematopoietic stem cell recruitment to retinal neovascularization sites, *Mol. Cell. Biochem.* 316 (2008) 177–186.
- [35] E. Padfield, H.P. Ellis, K.M. Kurian, Current therapeutic advances targeting EGFR and EGFRvIII in glioblastoma, *Front. Oncol.* 5 (2015) 5.
- [36] D.R. Leach, M.F. Krummel, J.P. Allison, Enhancement of antitumor immunity by CTLA-4 blockade, *Science* 271 (1996) 1734–1736.
- [37] S.J. Han, B.J. Ahn, J.S. Waldron, I. Yang, S. Fang, C.A. Crane, et al., Gamma interferon-mediated superinduction of B7-H1 in PTEN-deficient glioblastoma: a paradoxical mechanism of immune evasion, *Neuroreport* 20 (2009) 1597–1602.
- [38] R. Wilton, K. Burkhardt, V. Kindler, M.C. Belkouch, G. Dussex, N. Tribolet, et al., B7-homolog 1 expression by human glioma: a new mechanism of immune evasion, *Neuroreport* 16 (2005) 1081–1085.
- [39] A.T. Parsa, J.S. Waldron, A. Panner, C.A. Crane, I.F. Parney, J.J. Barry, et al., Loss of tumor suppressor PTEN function increases B7-H1 expression and immunoresistance in glioma, *Nat. Med.* 13 (2007) 84–88.
- [40] J. Chen, Y. Li, T.S. Yu, R.M. McKay, D.K. Burns, S.G. Kernie, et al., A restricted cell population propagates glioblastoma growth after chemotherapy, *Nature* 488 (2012) 522–526.
- [41] M. Zhang, R.L. Atkinson, J.M. Rosen, Selective targeting of radiation-resistant tumor-initiating cells, *Proc. Natl. Acad. Sci. U. S. A.* 107 (2010) 3522–3527.
- [42] V. Clement, P. Sanchez, N. de Tribolet, I. Radovanovic, A. Ruiz i Altaba, HEDGEHOG-GLI1 signaling regulates human glioma growth, cancer stem cell self-renewal, and tumorigenicity, *Curr. Biol.* 17 (2007) 165–172.
- [43] X. Fan, L. Khaki, T.S. Zhu, M.E. Soules, C.E. Talsma, N. Gul, et al., NOTCH pathway blockade depletes CD133-positive glioblastoma cells and inhibits growth of tumor neurospheres and xenografts, *Stem Cells* 28 (2010) 5–16.
- [44] M. Nager, D. Bhardwaj, C. Canti, L. Medina, P. Noguez, J. Herreros,  $\beta$ -Catenin signaling in glioblastoma multiforme and glioma-initiating cells, *Chemother. Res. Pract.* 2012 (2012) 192362.
- [45] S. Zhang, Y. Wang, J.H. Mao, D. Hsieh, I.J. Kim, L.M. Hu, et al., Inhibition of CK2 $\alpha$  down-regulates Hedgehog/Gli signaling leading to a reduction of a stem-like side population in human lung cancer cells, *PLoS One* 7 (2012) e38996.
- [46] A.H. Shih, E.C. Holland, Notch signaling enhances nestin expression in gliomas, *Neoplasia* 8 (2006) 1072–1082.
- [47] C.L. Calinescu, N. Kamran, G. Baker, Y. Mineharu, P.R. Lowenstein, M.G. Castro, Overview of current immunotherapeutic strategies for glioma, *Immunotherapy* 7 (2015) 1073–1104.
- [48] C.L. Efferson, C.T. Winkelmann, C. Ware, T. Sullivan, G.F. Draetta, et al., Downregulation of Notch pathway by a  $\gamma$ -secretase inhibitor attenuates AKT/mammalian target of rapamycin signaling and glucose uptake in an ERBB2 transgenic breast cancer model, *Cancer Res.* 70 (2010) 2476–2484.
- [49] D.H. Song, I. Dominguez, J. Mizuno, M. Kaut, S.C. Mohr, D.C. Seldin, CK2 phosphorylation of the armadillo repeat region of  $\beta$ -catenin potentiates Wnt signaling, *J. Biol. Chem.* 278 (2003) 24018–24025.
- [50] D.C. Seldin, E. Landesman-Bollag, M. Farago, N. Currier, D. Lou, I. Dominguez, CK2 as a positive regulator of Wnt signalling and tumorigenesis, *Mol. Cell. Biochem.* 274 (2005) 63–67.
- [51] R.T. Nitta, S. Gholamin, A.H. Feroze, M. Agarwal, S.H. Cheshier, S.S. Mitra, et al., Casein kinase 2 $\alpha$  regulates glioblastoma brain tumor-initiating cell growth through the  $\beta$ -catenin pathway, *Oncogene* 34 (2015) 3688–3699.
- [52] X. Jin, J. Yin, S.H. Kim, Y.W. Sohn, S. Beck, Y.C. Lim, et al., EGFR-AKT-Smad signaling promotes formation of glioma stem-like cells and tumor angiogenesis by ID3-driven cytokine induction, *Cancer Res.* 71 (2011) 7125–7134.
- [53] X. Yue, F. Lan, W. Yang, Y. Yang, L. Han, A. Zhang, et al., Interruption of  $\beta$ -catenin suppresses the EGFR pathway by blocking multiple oncogenic targets in human glioma cells, *Brain Res.* 1366 (2010) 27–37.
- [54] T. Ashizawa, H. Miyata, A. Iizuka, M. Komiya, C. Oshita, A. Kume, et al., Effect of the STAT3 inhibitor STX-0119 on the proliferation of cancer stem-like cells derived from recurrent glioblastoma, *Int. J. Oncol.* 43 (2013) 219–227.